

Vacancy complexes in nonequilibrium germanium-tin semiconductors

Assali, S.; Elsayed, M.; Nicolas, J.; Liedke, M. O.; Wagner, A.; Butterling, M.; Krause-Rehberg, R.; Moutanabbir, O.;

Originally published:

June 2019

Applied Physics Letters 114(2019), 251907

DOI: <https://doi.org/10.1063/1.5108878>

Perma-Link to Publication Repository of HZDR:

<https://www.hzdr.de/publications/Publ-29385>

Release of the secondary publication
on the basis of the German Copyright Law § 38 Section 4.

Vacancy complexes in nonequilibrium germanium-tin semiconductors

S. Assali,^{1,*} M. Elsayed,^{2,3} J. Nicolas,¹ M. O. Liedke,⁴ A. Wagner,⁴ M. Butterling,⁴ R. Krause-Rehberg,² and O. Moutanabbir^{1,*}

¹Department of Engineering Physics, École Polytechnique de Montréal, C. P. 6079, Succ. Centre-Ville, Montréal, Québec H3C 3A7, Canada

²Martin Luther University Halle, 06099 Halle, Germany

³Department of Physics, Faculty of Science, Minia University, 61519 Minia, Egypt

⁴Helmholtz-Zentrum Dresden-Rossendorf, Institute of Radiation Physics, Bautzner Landstraße 400, 01328 Dresden, Germany

Depth-profiled pulsed low-energy positron annihilation lifetime spectroscopy and Doppler broadening spectroscopy were combined to identify vacancy-related complexes and probe their evolution as a function of Sn content in GeSn epitaxial layers. Regardless of the Sn content in the 6.5-13.0 at.% range, all GeSn samples showed the same depth-dependent increase in the positron annihilation line broadening parameters, relative to that of epitaxial and bulk Ge references thus confirming the formation of open volume defects during growth. The measured average positron lifetimes were found to be the highest (380-395 ps) in the region near the surface and monotonically decrease across the analyzed thickness, but remain above 350 ps. All GeSn layers exhibit average lifetimes that are 20 to 160 ps higher than those recorded for the Ge reference. Surprisingly, these lifetimes were found to decrease as Sn content increases in GeSn layers. These measurements indicate that divacancies are the dominant defect in the as-grown GeSn layers. However, their corresponding lifetime was found to be shorter than in epitaxial Ge thus suggesting that the presence of Sn may alter the structure of divacancies. Additionally, GeSn layers were found to also contain a small fraction of vacancy clusters, which become less important as Sn concentration increases. The interaction and possible pairing between Sn and vacancies have been proposed to explain the reduced formation of larger vacancy clusters in GeSn when Sn content increases.

Developing opto-electronic devices on silicon provides a viable path for monolithic manufacturing of photonic integrated circuits with significant cost reduction and new functionalities for a wide range of applications.¹ In this regard, GeSn has been suggested as potential building blocks for silicon-compatible light sources.² This material system provides two degrees of freedom for band structure engineering, namely, alloying and strain. This characteristic is central to engineer novel low-dimensional systems and heterostructures in a similar fashion to III-V semiconductors. Moreover, a direct band gap can be obtained in GeSn which is promising for efficient emission and detection of light.³⁻⁵ The flexibility in band gap engineering provided by these group IV semiconductors has sparked a recent surge of interest in the growth of device quality layers on Si or Ge substrates.⁶⁻⁹ However, the epitaxial growth of GeSn semiconductors has been proven to be very challenging due to the low equilibrium solubility of Sn in Si (<0.1at.%) and Ge (<1at.%). Additionally, above 13.2°C the semiconducting α -Sn phase (diamond structure) transforms into metallic β -Sn phase.

Despite the long list of the growth hurdles, the recent progress in controlling the growth kinetics overcame these difficulties leading to the epitaxial growth of device-quality layers with high Sn content.⁶⁻¹⁰ However, to avoid surface segregation and phase separation, the growth is typically carried out below 400°C, thus raising fundamental questions regarding point defects that are inherent to low growth temperatures. In fact, this reduced temperature is likely to limit the mobility of the deposited species to an extent of hindering the long-range growth ordering and yielding an increase in vacancy trapping. Native point defects such as vacancies and vacancy complexes can greatly impact the microstructure and the electronic properties of the epitaxial layers. Vacancies can promote the motion and interaction of dislocations, thus impacting both the density and the type of extended defects.¹¹ Moreover, vacancy-related lattice defects can also

significantly limit the efficiency of light emission and detection via doping compensation and carrier trapping.¹²⁻¹⁴ Despite their importance, studies of the vacancy-related complexes in epitaxial Sn-containing group IV semiconductors are still conspicuously missing in literature. With this perspective, this work reports on the direct analysis of vacancy complexes and elucidates their behavior as a function of the Sn content in metastable GeSn epitaxial layers. By combining depth-profiled positron annihilation lifetime spectroscopy (PAS) and Doppler broadening measurements, we found that divacancy is the dominant complex observed in GeSn layers independently of Sn content, while only a small fraction of larger vacancy clusters was observed. Intriguingly, the increase in Sn incorporation was found to be associated with a slight increase in divacancies and concomitant decrease in vacancy clusters.

The investigated samples were grown on a 4-inch Si (100) wafers in a low-pressure chemical vapor deposition (CVD) reactor using ultra-pure H₂ carrier gas, 10% monogermane (GeH₄) and tin-tetrachloride (SnCl₄) precursors.^{8,10,15} First, a 500-700nm-thick Ge/Si virtual substrate (Ge-VS) was grown at 450°C, followed by thermal cyclic annealing (>800°C) and additional Ge deposition. Next, a 500-700nm-thick GeSn layer (Fig.1a) was grown at a fixed temperature in the 330-300°C range, corresponding to 6.5-13at.% Sn content, as estimated from Reciprocal Space Mapping (RSM) X-ray diffraction (XRD) measurements (Fig.1a-inset and (Supporting Information S1). Herein, the highest Sn content is obtained at the lowest growth temperature and *vice versa*.^{10,15} The residual (compressive) in-plane strain in the GeSn layers being lower than -0.3% allows for a direct comparison in the 2 θ - ω scans around the (004) XRD order in Fig.1b, where a shift of the GeSn peak toward lower angles with increasing Sn content is observed.¹⁰ Doppler broadening analyses were carried out using a variable energy positron beam of 0.03–35keV. This energy range corresponds to a mean penetration depth reaching ~2 μ m, thus

ensuring that the entire thickness of GeSn layers (700nm) is probed. The Doppler broadening spectrum of the 511keV annihilation line is characterized by two parameters, S (low-electron momentum fraction) and W (high-electron momentum fraction). The trapping of positrons at open-volume defects is detected as an increase in S -parameter (decrease W -parameter).¹⁶ PAS lifetime measurements were performed using the mono-energetic positron source (MePS) at the superconducting electron linear accelerator ELBE located at the Helmholtz-Zentrum Dresden-Rossendorf (Supporting Information S2).^{17,18}

The evolution of the S -parameter as a function of the positron energy in each GeSn layer is shown in Fig.2 and compared to measurements performed on Ge bulk and 600nm-thick epilayer references. It is noticeable that the S -parameter increases as the positron energy increases up to 10keV ($z_{\text{mean}} \sim 310\text{nm}$). At higher depths ($E > 12\text{keV}$), the positron beam reaches the Si wafer and a constant value of $S \sim 0.52$ is recorded. All GeSn samples show a similar trend. The S -parameter is larger than in the case of the Ge-VS up to 10keV ($z_{\text{mean}} \sim 310\text{nm}$), followed by a progressive decrease reaching the Si value at 30keV ($z_{\text{mean}} \sim 2000\text{nm}$). We note that despite the use of higher energies, the interaction of the positron beam with the GeSn layers induced by the broadening of the Makhov profile,¹⁹ leads to S -parameter values in the underlying Ge-VS larger than in the reference layer without GeSn. Fig.1b displays the S -parameter for GeSn layers and Ge-VS normalized to that of bulk Ge ($S/S_{\text{Ge-bulk}}$). An increase in the normalized $S/S_{\text{Ge-bulk}}$ parameter results from the reduced diffusion length of the positrons due to an increased density of defects.^{20,21} Thus, a higher amount of open-volume defects is observed when moving from the surface of the GeSn layer down to the interface with the Ge-VS. As a simple approximation, when the defect concentrations does not vary significantly, S -parameter values of 1.030, 1.034–1.044, 1.05–1.07, and 1.10–1.14 are expected for monovacancies, divacancies, small vacancy clusters, and voids,

respectively.^{16,22,23} Therefore, the data in Fig.2b provide the first hint that the predominant defects in as-grown GeSn layers are likely divacancies and vacancy clusters, as confirmed below.

The positron lifetime measurements as a function of depth are exhibited in Fig.3a. In the Ge-VS, the average lifetime τ_{AV} drops from 360ps near the surface down to 315ps at the interface with the Si substrate. Independently of the probed depth, τ_{AV} is well above that of the bulk Ge $\tau_b=224-228ps$,^{24,25} thus confirming that vacancy-related defects are present in the Ge-VS. For GeSn layers, a decrease in τ_{AV} with increasing depth is observed in all samples. It is noticeable that the incorporation of Sn is always associated with an increase in the average lifetime as compared to Ge-VS, but with a less pronounced decrease as a function of depth. τ_{AV} at various depths as a function of Sn content is displayed in Fig.3b. Surprisingly, the sample with the highest Sn content (13at.%) always shows the shortest τ_{AV} across the whole thickness. At a first glimpse, this observation seems rather counterintuitive as the layers with the highest Sn content were grown at a slightly lower temperature (300°C), which should further promote the formation of vacancies. As it will be discussed later, a possible interaction between Sn and vacancy complexes can be invoked to explain this behavior.

To investigate the nature of the detected open volume defects, the lifetime spectra were fitted with two lifetime components.¹⁶ For the reference Ge-VS, the results for the lifetimes τ_1 and τ_2 and the intensities I_1 and I_2 are plotted as a function of the mean depth in Fig.4. The intensity for the long-lived component I_2 is always higher (55-75%) than the short-lived one I_1 across the whole thickness. Interestingly, τ_1 values are in the 250-225ps range, hence at much shorter-lived values compared to the 405-350ps range observed for τ_2 . The calculated lifetime values in bulk Ge for the isolated vacancy is 263ps, while for divacancies the lifetime increases to 325ps.²⁴

Experimentally, the reference bulk Ge lifetime is $\tau_b=224-228\text{ps}$,^{24,25} thus the τ_1 values are approaching the defect-free bulk lifetime. This lifetime seems to be consistent with positron trapping in dislocations.^{26,27} Note that Ge-VS is grown on Si and thus it contains a relatively large density of threading dislocations ($>10^7/\text{cm}^2$). A $\tau_2>330\text{ps}$ was recorded for neutral divacancy in bulk Ge samples irradiated with neutrons,²⁸ while values below 320ps are generally associated with negatively charged divacancies, which results in a background p-type doping in Ge.¹³ In proton-irradiated Ge bulk samples, vacancy-like defects with a negative charge state and a lifetime of 294ps, assigned as V-As complexes, were also reported.²⁹ However, it is noteworthy that monovacancies are usually measurable only below 200K, since above this temperature neutral monovacancies pair to form divacancies.³⁰ In addition, clusters formed by 3 or more vacancies are associated with a lifetime longer than 365ps.³¹ The deconvoluted lifetime results in Fig.4 shows that clusters made of multiple vacancies³⁰ are present with a $\tau_2=405-350\text{ps}$. Thus, the higher growth (450°C) and thermal cyclic annealing ($>800^\circ\text{C}$) temperatures seem to annihilate most of the divacancies, while the remaining ones tend to form vacancy clusters. This is consistent with an early report on divacancy clustering in neutron-irradiated Ge.²⁴

The results for the τ_1 , τ_2 lifetimes and their corresponding I_1 , I_2 intensities as a function of the mean depth for the 13at.% Sn sample are plotted in Fig.5a-b. Note that in the samples with lower Sn contents, the analysis yields qualitatively the same behavior. The shortest lifetime τ_1 decreases from 366ps near GeSn surface (20nm) to 324ps at the interface with the Ge-VS (623nm). A striking difference is, however, observed for the second lifetime τ_2 , where much larger values ranging from 490ps to 750ps are obtained. The surface and defective interface act as a sink for vacancies, meaning that vacancies can diffuse and anneal out close to these regions. As these vacancies diffuse toward the surface or GeSn/Ge interface, they can also interact and form even

larger clusters or voids. This translates by an increase in the lifetime close to these regions. It is remarkable that, across the whole layer thickness, the shortest lifetime τ_1 dominates by far the recombination process, with an intensity I_1 higher than 80%. As a result, the longer τ_2 component induces only a small increase in the average lifetime τ_{AV} .

The effect of the GeSn alloy composition on the intensity and lifetime recorded at a randomly fixed depth of 215nm is shown in Fig.5c-d. The intensity I_1 increases from 65% to 83% with increasing Sn content, while the shortest lifetime τ_1 remains constant at 335 ± 2 ps. At the same time, the longer lifetime τ_2 increases slightly from 469ps to 489ps. In GeSn the shortest lifetime $\tau_1=335$ ps can be associated with the presence of divacancies in the GeSn layer, while the longest lifetime $\tau_2>450$ ps is associated with clusters made of multiple vacancies, most likely with more than 5 vacancies.³⁰ However, the intensity I_2 being much lower than I_1 demonstrates that the concentration of vacancy-clusters is rather low compared to that of divacancies. Indeed, the increase of intensity I_1 with Sn content, reaching 80% at 13at.% of Sn (Fig.5c), indicates that divacancies are the predominant type of point defects in GeSn. This result also provides clear evidence that divacancy is stable in GeSn at room-temperature, which is the temperature at which PAS measurements were conducted. The composition of GeSn alloys was controlled during growth by decreasing the temperature from 330°C(6.5at.%) to 300°C(13at.%), which may limit the mobility of vacancy complexes during growth and consequently their interaction can become less probable, thus reducing the likelihood of the formation of larger vacancy clusters. However, the reduction in growth temperature is too small to significantly impact the dynamics of vacancy complexes and their interactions, where activation energies above 1eV characterize the migration processes of divacancies in Ge.³²

As mentioned above, τ_1 does not depend on the Sn composition in the investigated range and is always more than 85ps above the 250-225ps recorded for Ge-VS. This may suggest that the divacancy structure is perhaps altered by the presence of Sn and the associated lattice stress. It is reasonable to believe that because the Sn atom is larger than Ge atom the pairing of Sn with vacancies would be a viable path to locally minimize the stress associated with Sn incorporation. It is currently well established that Sn occupies substitutional sites in GeSn lattice and is randomly distributed⁸ with no sign of any short-range ordering.³³ However, early reports on the interaction of Sn with simple defects in irradiated Ge provided evidence of an affinity of Sn atoms to attract vacancies in order to relieve the stress in Ge lattice.³⁴ This attractive interaction between Sn and vacancies was also suggested based on *ab initio* calculations combined with emission channeling studies of Sn-implanted Ge.³⁵ Based on thermodynamic considerations, these studies confirmed that the isovalent Sn expectedly favors substitutional sites, but it can also trap vacancies and then the Sn atom occupies the bound centered site under vacancy-split configuration. Note that Sn-divacancy complexes in irradiated Ge were shown to anneal out at 220K,³⁶ which is significantly below the temperatures of growth and PAS measurements used in this study. Nevertheless, the formation of these complexes in epitaxial films cannot be ruled out as the growth kinetics can affect their thermal stability. Our lifetime measurements agree, at least qualitatively, with the aforementioned observations, and indicate a possible effect of Sn that can locally *freeze* vacancies, thus limiting their clustering during growth. Indeed, the observed drop in the intensity of vacancy clusters I_2 as Sn content increases underscores a certain role of Sn in reducing vacancy migration and interaction to form clusters, leading to a decrease in τ_{AV} as the long-lived τ_2 component becomes less important at higher Sn incorporation. Finally, it is important to emphasize that dislocations in the proximity of the GeSn-Ge interface^{8,10} do not have an impact on Doppler

ing, ordering and lifetime measurements. Vacancy-free dislocations would act as shallow positron traps only at low temperatures ($T < 100\text{K}$), hence irrelevant under our conditions, while they show a lifetime close to the bulk value at 300K . If dislocations contain vacancies, they would act as deep positron trap, leading a lifetime below 300ps . Here, the experimental lifetime recorded above 320ps excludes the presence of monovacancies in GeSn at room-temperature.

In summary, vacancy-related complexes were investigated in GeSn semiconductors at Sn content in the $6.5\text{-}13.0\text{at.}\%$ range using positron annihilation spectroscopies. These studies confirm the presence of open volume defects in GeSn layers. A monotonic decrease in the measured lifetime from $380\text{-}395\text{ps}$ (close to the sample surface) down to 350ps (proximity of the Ge-VS) was recorded across the GeSn thickness. When compared to Ge reference, the measured average lifetimes in GeSn were found to be 20 to 160ps higher. In addition, the average lifetime was also found to be inversely proportional to Sn content in the GeSn layers. These results demonstrate that divacancies are the dominant defects in the as-grown GeSn layers, while only a small fraction of vacancy clusters is present in the alloy. A possible attractive interaction between Sn and vacancies has been suggested to explain the reduced clustering of vacancies in GeSn as Sn content increases.

FIGURES CAPTIONS

Figure 1. (a) Cross-sectional TEM image along the $[110]$ zone axis. Inset: (224) -RSM map for the $13\text{at.}\%$ GeSn sample showing the graded ($<12.9\text{at.}\%$) and uniform ($13.7\text{at.}\%$) composition. (b) 2θ - ω scans around the (004) -XRD order acquired on the $6.5\text{-}13\text{at.}\%$ GeSn samples (grown at $330\text{-}300^\circ\text{C}$) and the Ge-VS substrate (grown at 450°C , annealed $>800^\circ\text{C}$).

Figure 2.(a)S-parameter as a function of the incident positron energy for all GeSn samples and for the reference Ge-VS.(b)Normalized $S/S_{\text{Ge-bulk}}$ parameter as a function of the incident positron energy for all GeSn samples. The penetration depth of the positron beam was estimated at different energies using Ge lattice as a reference.

Figure 3.(a)Average lifetime τ_{AV} as a function of the positron mean depth for all GeSn and Ge-VS samples.(b) τ_{AV} as a function of the Sn content for different positron mean depths.

Figure 4.(a-b)Decomposition of the intensity(a) and lifetime(b) spectra as a function of the positron mean depth for the Ge-VS sample.

Figure 5.(a-b)Decomposition of the intensity(a) and lifetime(b) spectra as a function of the positron mean depth in 13at.% GeSn.(c-d)Decomposition of the intensity(c) and lifetime(d) spectra as a function of the composition at a depth of 215nm.

SUPPLEMENTARY MATERIAL

See supplementary material for additional information on the XRD-RSM characterization and on the Doppler broadening and PAS measurements.

ACKNOWLEDGMENTS

The authors thank J. Bouchard for the technical support with the CVD system. O.M. acknowledges support from NSERC Canada (Discovery, SPG, and CRD Grants), Canada Research Chairs, Canada Foundation for Innovation, Mitacs, PRIMA Québec, and Defence Canada (Innovation for Defence Excellence and Security, IDEaS). S.A. acknowledges support from Fonds de recherche du Québec-Nature et technologies (FRQNT, PBEEE scholarship). Positron annihilation

experiments were carried out in the ELBE facility thanks to the large infrastructure program of the EU (proposal no. POS18101148). We acknowledge BMBF for the PosiAnalyse (05K2013) grant, the Impulse- und Networking fund of the Helmholtz-Association (FKZ VH-VI-442 Memriox), and the Helmholtz Energy Materials Characterization Platform (03ET7015).

AUTHOR INFORMATION

Corresponding Authors:

*E-mail: simone.assali@polymtl.ca

*E-mail: oussama.moutanabbir@polymtl.ca

Notes:

The authors declare no competing financial interest.

REFERENCES

- ¹ L. Pavesi and D.J. Lockwood, editors, *Silicon Photonics III: Systems and Applications* (Springer Berlin Heidelberg, Berlin, Heidelberg, 2016).
- ² R. Soref, *Nat. Photonics* **4**, 495 (2010).
- ³ S. Gupta, B. Magyari-Köpe, Y. Nishi, and K.C. Saraswat, *J. Appl. Phys.* **113**, (2013).
- ⁴ A. Attiaoui and O. Moutanabbir, *J. Appl. Phys.* **116**, 063712 (2014).
- ⁵ M.P. Polak, P. Scharoch, and R. Kudrawiec, *J. Phys. D. Appl. Phys.* **50**, 195103 (2017).
- ⁶ S. Wirths, R. Geiger, N. von den Driesch, G. Mussler, T. Stoica, S. Mantl, Z. Ikonic, M. Luysberg, S. Chiussi, J.M. Hartmann, H. Sigg, J. Faist, D. Buca, and D. Grützmacher, *Nat. Photonics* **9**, 88 (2015).
- ⁷ J. Aubin, J.M. Hartmann, A. Gassenq, J.L. Rouviere, E. Robin, V. Delaye, D. Cooper, N. Mollard, V. Reboud, and V. Calvo, *Semicond. Sci. Technol.* **32**, 094006 (2017).
- ⁸ S. Assali, J. Nicolas, S. Mukherjee, A. Dijkstra, and O. Moutanabbir, *Appl. Phys. Lett.* **112**,

151903 (2018).

⁹ W. Dou, M. Benamara, A. Mosleh, J. Margetis, P. Grant, Y. Zhou, S. Al-Kabi, W. Du, J. Tolle, B. Li, M. Mortazavi, and S.-Q. Yu, *Sci. Rep.* **8**, 5640 (2018).

¹⁰ S. Assali, J. Nicolas, and O. Moutanabbir, *J. Appl. Phys.* **125**, 025304 (2019).

¹¹ D. Hull and D.J. Bacon, *Introduction to Dislocations* (Elsevier, 2011).

¹² W.P. Bai, N. Lu, A. Ritenour, M.L. Lee, D.A. Antoniadis, and D.-L. Kwong, *IEEE Electron Device Lett.* **27**, 175 (2006).

¹³ M. Christian Petersen, A. Nylandsted Larsen, and A. Mesli, *Phys. Rev. B* **82**, 075203 (2010).

¹⁴ C.G. Van de Walle and J. Neugebauer, *J. Appl. Phys.* **95**, 3851 (2004).

¹⁵ É. Bouthillier, S. Assali, J. Nicolas, and O. Moutanabbir, *Arxiv.Org/Abs/1901.00436* (2019).

¹⁶ O. Moutanabbir, R. Scholz, U. Gösele, A. Guittoum, M. Jungmann, M. Butterling, R. Krause-Rehberg, W. Anwand, W. Egger, and P. Sperr, *Phys. Rev. B* **81**, 115205 (2010).

¹⁷ M.O. Liedke, W. Anwand, R. Bali, S. Cornelius, M. Butterling, T.T. Trinh, A. Wagner, S. Salamon, D. Walecki, A. Smekhova, H. Wende, and K. Potzger, *J. Appl. Phys.* **117**, 163908 (2015).

¹⁸ W. Anwand, G. Brauer, M. Butterling, H.R. Kissener, and A. Wagner, *Defect Diffus. Forum* **331**, 25 (2012).

¹⁹ A.F. Makhov, *Sov. Phys.-Solid State* **2**, (1934).

²⁰ M. Elsayed, R. Krause-Rehberg, B. Korff, S. Richter, and H.S. Leipner, *J. Appl. Phys.* **113**, 094902 (2013).

²¹ E. Kamiyama, S. Nakagawa, K. Sueoka, T. Ohmura, T. Asano, O. Nakatsuka, N. Taoka, S. Zaima, K. Izunome, and K. Kashima, *Appl. Phys. Express* **7**, 021302 (2014).

²² P.J. Schultz and K.G. Lynn, *Rev. Mod. Phys.* **60**, 701 (1988).

²³ F. Tuomisto and I. Makkonen, *Rev. Mod. Phys.* **85**, 1583 (2013).

²⁴ K. Kuitunen, F. Tuomisto, J. Slotte, and I. Capan, *Phys. Rev. B* **78**, 033202 (2008).

²⁵ J. Slotte, S. Kilpeläinen, F. Tuomisto, J. Räisänen, and A.N. Larsen, *Phys. Rev. B* **83**, 235212 (2011).

²⁶ E. Kuramoto, S. Takeuchi, M. Noguchi, T. Chiba, and N. Tsuda, *Appl. Phys.* **4**, 41 (1974).

²⁷ Y. Kamimura, T. Tsutsumi, and E. Kuramoto, *Phys. Rev. B* **52**, 879 (1995).

²⁸ J. Slotte, K. Kuitunen, S. Kilpeläinen, F. Tuomisto, and I. Capan, *Thin Solid Films* **518**, 2314 (2010).

²⁹ M. Elsayed, N. Yu. Arutyunov, R. Krause-Rehberg, V.V. Emtsev, G.A. Oganessian, and V.V. Kozlovski, *Acta Mater.* **83**, 473 (2015).

³⁰ M. Elsayed, N.Y. Arutyunov, R. Krause-Rehberg, G.A. Oganessian, and V.V. Kozlovski, *Acta Mater.* **100**, 1 (2015).

³¹ R. Krause-Rehberg, M. Brohl, H.S. Leipner, T. Drost, A. Polity, U. Beyer, and H. Alexander, Phys. Rev. B **47**, 13266 (1993).

³² C. Janke, R. Jones, S. Öberg, and P.R. Briddon, Phys. Rev. B **75**, 195208 (2007).

³³ S. Mukherjee, N. Kodali, D. Isheim, S. Wirths, J.M. Hartmann, D. Buca, D.N. Seidman, and O. Moutanabbir, Phys. Rev. B **95**, 161402 (2017).

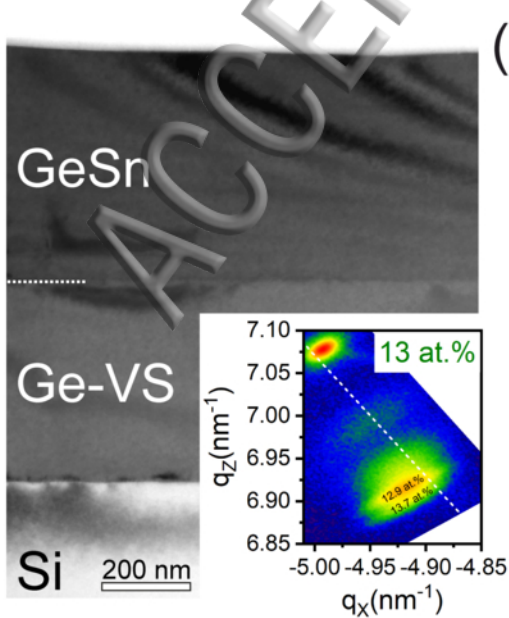
³⁴ I. Riihimäki, A. Virtanen, H. Kettunen, P. Pusa, P. Laitinen, J. Räisänen, and the ISOLDE Collaboration, Appl. Phys. Lett. **90**, 181922 (2007).

³⁵ S. Decoster, S. Cottenier, U. Wahl, J.G. Correia, and A. Vantomme, Phys. Rev. B **81**, 155204 (2010).

³⁶ L.I. Khirunenko, M.G. Sosnin, A. V. Duvanskii, N. V. Abrosimov, and H. Riemann, J. Appl. Phys. **123**, 1 (2018).

ACCEPTED MANUSCRIPT

(a)



(b)

